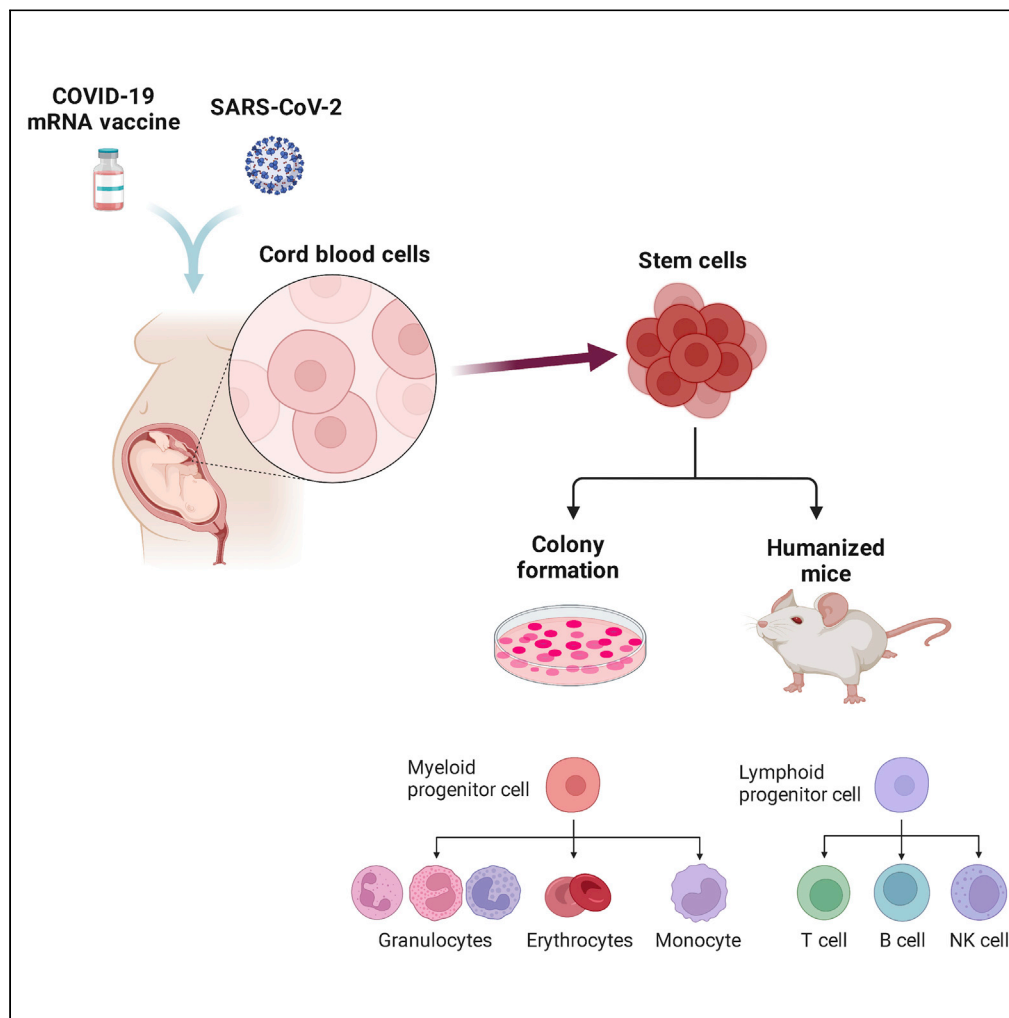## Article

Skewed fate and hematopoiesis of CD34$^+$ HSPCs in umbilical cord blood amid the COVID-19 pandemic

Benjamin K. Estep, Charles J. Kuhlmann, Satoru Osuka, ..., Chloe E. Jepson, Paul A. Goepfert, Masakazu Kamata

masa3k@uab.edu

Highlights

SARS-CoV-2 infection/ vaccination correlate with the *in vivo fate of* CD34$^+$ HSPCs

SARS-CoV-2 infection/ vaccination correlate with hematopoiesis of CD34$^+$ HSPCs

SARS-CoV-2 vaccination correlates with CD34$^+$ HSPC numbers/ frequencies in the UCB

iScience

Article

Skewed fate and hematopoiesis of CD34$^+$ HSPCs in umbilical cord blood amid the COVID-19 pandemic

Benjamin K. Estep,[1] Charles J. Kuhlmann,[1] Satoru Osuka,[4] Gajendra W. Suryavanshi,[5] Yoshiko Nagaoka-Kamata,[2] Ciearria N. Samuel,[1] Madison T. Blucas,[1] Chloe E. Jepson,[1] Paul A. Goepfert,[3] and Masakazu Kamata[1,6,*]

SUMMARY

Umbilical cord blood (UCB) is an irreplaceable source for hematopoietic stem progenitor cells (HSPCs). However, the effects of SARS-CoV-2 infection and COVID-19 vaccination on UCB phenotype, specifically the HSPCs therein, are currently unknown. We thus evaluated any effects of SARS-CoV-2 infection and/or COVID-19 vaccination from the mother on the fate and functionalities of HSPCs in the UCB. The numbers and frequencies of HSPCs in the UCB decreased significantly in donors with previous SARS-CoV-2 infection and more so with COVID-19 vaccination via the induction of apoptosis, likely mediated by IFN-γ-dependent pathways. Two independent hematopoiesis assays, a colony forming unit assay and a mouse humanization assay, revealed skewed hematopoiesis of HSPCs obtained from donors delivered from mothers with SARS-CoV-2 infection history. These results indicate that SARS-CoV-2 infection and COVID-19 vaccination impair the functionalities and survivability of HSPCs in the UCB, which would make unprecedented concerns on the future of HSPC-based therapies.

INTRODUCTION

Umbilical cord blood (UCB) is the blood originating from the neonate.[1,2] UCB differs from that of adult peripheral blood, in which UCB contains higher numbers of monocytes and nucleated red blood cells (RBCs), and lower numbers of matured RBCs and T cells, especially CD8$^+$T cells.[3,4] Lymphocytes in UCB produce fewer absolute levels of cytokines and have higher abundance of anti-inflammatory cytokines than adult peripheral blood sources. More importantly, UCB is highly enriched with multipotent hematopoietic stem progenitor cells (HSPCs) as identified by the surface expression of CD34 molecules, which are essential for the maintenance of the bone marrow and blood systems[5]; HSPCs have been widely used for various therapeutic and research purposes, such as bone marrow transplants[6,7] and the treatment of severe cases of COVID-19.[8,9] However, the fate and functionality of CD34$^+$ HSPCs are severely affected by the host's health status, such as infection by a pathogen, which can cause stress-induced hematopoiesis in these HSPCs.[10,11]

The novel Coronavirus disease 2019 (COVID-19) is the result of infection by the severe acute respiratory syndrome-related coronavirus 2 (SARS-CoV-2).[12,13] The disease is not limited to acute respiratory pathology, but can also induce a systemic, long-term pathology called 'long- (or post-) COVID syndrome'.[14–16] Highly effective vaccines against SARS-CoV-2, so-called COVID-19 vaccines, were deployed at the end of 2020,[17] which prevent infection of some SARS-CoV-2 strains and severe disease. However, there are few reports addressing the potential risk(s) of the infection in conjunction with vaccination on the fetus and neonate via the mother.[18–22]

Little is known about the impacts of previous SARS-CoV-2 infection, including asymptomatic infection, and/or COVID-19 vaccination on the functionality of CD34$^+$ HSPCs.[23,24] In general, HSPCs are considered as one of the first responders to infection as well as vaccination which include releasing pro-inflammatory cytokines, such as type I and II interferons (IFNs), tumor necrosis factor (TNF), interleukin (IL)-1, 6, and 8; all of which are crucially important for functional regulation of HSPCs.[25] Infection of CD34$^+$ HSPCs by

[1]Department of Microbiology, University of Alabama at Birmingham, 845 19th Street South, Birmingham, AL 35205, USA

[2]Department of Pathology, University of Alabama at Birmingham, Birmingham, AL 35205, USA

[3]Department of Medicine and Division of Infectious Diseases, School of Medicine, University of Alabama at Birmingham, Birmingham, AL 35205, USA

[4]Department of Neurosurgery, School of Medicine, University of Alabama at Birmingham, Birmingham, AL 35233, USA

[5]Division of Microbiology, Immunology and Molecular Genetics, David Geffen School of Medicine at UCLA, Los Angeles, CA 90095, USA

[6]Lead contact

*Correspondence: masa3k@uab.edu

https://doi.org/10.1016/j.isci.2022.105544

SARS-CoV-2 *in vitro* displayed reduced hematopoietic colony formation potential and an increased potential for erythrocyte and thrombocyte precursors as well as higher susceptibility to apoptosis.[26,27] However, these studies have not clarified or demonstrated the long-term effects of SARS-CoV-2 infection on CD34^{+} cell functionalities *in vivo* nor CD34^{+} HSPCs in the UCB obtained from the neonate delivered from pregnant women who were asymptomatically infected by SARS-CoV-2 and/or vaccinated. Importantly, SARS-CoV-2 infections during pregnancy can cause significant adverse effects on the newborn's health status, development, and prematurity; these complications are thought to be the result of immune reactions and hematopoietic dysregulation within the mother and developing fetus.[18,28–36] Similarly, SARS-CoV-2 mRNA vaccines also include an identical concern because they induce a unique but dynamic immune response.[37] Thus, the immune responses and cytokine profiles in pregnant women who were infected by SARS-CoV-2 and/or vaccinated against SARS-CoV-2 indicate a concern in the maintenance and proper functions and phenotypes of HSPCs in the UCB as well as hematopoiesis in the fetus and neonate.

Here, the impact of previous SARS-CoV-2 infection, specifically asymptomatic or undocumented infection, and COVID-19 vaccination on CD34^{+} HSPCs in UCB was investigated. A total of 111 UCB donor samples from Alabama were eligible and/or tested for the assays as shown in Table S1. Striking changes were observed in the CD34^{+} cell fraction: the total numbers of CD34^{+} cells drastically reduced 4-fold in the vaccinated donor group, in which this change was correlated with the induction of apoptosis in CD34^{+} cells, likely mediated by IFN-γ-related pathways as determined by a total transcriptome assay. In addition, the hematopoietic abilities of these CD34^{+} cells showed skewing in two different hematopoiesis assays – an *in vitro* colony-formation unit (CFU) and a mouse humanization assay – as represented by high T cell/B cell ratios and higher erythrocyte and lower granulocyte-macrophage colony formations. These data indicate that both previous SARS-CoV-2 infection and/or vaccination impair CD34^{+} HSPCs quantitatively and qualitatively by stress-induced hematopoiesis, which is a great concern in the collection as well as the utilization of UCB as a source of CD34^{+} HSPCs used in/for future therapies, treatments, and research.

RESULTS

Both previous-SARS-CoV-2 infection and vaccination negatively impact CD34^{+} HSPC frequencies and numbers in the UCB

Several features of cord blood are affected by external or maternal factors, such as maternal age, gestation period length, the mother's age, or the baby's weight.[38,39] Table S1 shows the enrolled eligible donor population used for the research. The donors were primarily classified into three groups, including 5 subcategories, by the presence or absence of IgGs specific for SARS-CoV-2 nucleocapsid (N) and spike (S) proteins in the UCB plasma because a significant number of people are asymptomatically infected by this virus[40] and official vaccination history/cards: (1) *Negative group* (n = 39, N-/S-) has no medical history for the infection nor vaccination and no detectable anti-S or N IgGs (N-/S-) in the UCB plasma, (2) *Non-vaccinated group* (n = 40) has no medical history for the infection and vaccination, but were positive for IgGs against either only S protein (n = 21, N-/S+) or both N and S proteins (n = 19, N+/S+), (i.e., including donors only asymptomatically infected) and (3) *Vaccinated group* (n = 32) is the same as the second group but has a medical record for vaccination (n = 21, N-/S+ and n = 11, N+/S+), (i.e., including donors asymptomatically infected and/or vaccinated). The differences seen in the presence of these IgGs can be used to estimate the timing of the infection because the half-life of anti-S IgG in the previously infected individuals is more than double compared to that of anti-N IgG,[27,41,42] indicating that the donors single positive for anti-S IgG were infected far before the donors double-positive for anti-S and N IgGs. There were no donors single positive for anti-N IgG only in all 111 eligible donor samples. UCB samples were obtained between March 18th and December 15th, 2021, when vaccination rates were consistently high in Alabama.

No significant difference in the baby's weight at term as well as the volume of UCB were observed between groups, but the numbers of mononucleated cells (MNC) decreased in the non-vaccinated and vaccinated donor groups, even so more in combination with the vaccination and the presence of anti-N IgG more than 2-fold compared to the negative donor group (624 × 10^{6} MNCs versus 287 × 10^{6} MNCs, Table S1 and Figure S1). Flow cytometrical analysis of the whole UCB using a gating strategy as shown in Figure S2 indicated little variations or differences in any specific lymphocyte population frequencies/numbers, even though some moderate variations were observed (Figure S3), indicating that the decrease in the MNC numbers cannot be solely explained by changes in specific blood immune cell types. Because MNCs are all derived from CD34^{+} HSPCs, any changes in the CD34^{+} cell population in the MNC fractions were assessed further using a gating strategy as shown in Figure S4. A striking difference was observed in both the % frequency

and the total estimated number of CD34+ cells per 1 mL of UCB: both parameters decreased 1.7 to 3-fold in the non-vaccinated and vaccinated donor groups, respectively, compared to the negative donor group, regardless of the positivity for IgGs against SARS-CoV-2 S and N proteins (Figures 1A and 1B).

To assess the recovery time needed for decreased CD34+ cell numbers of donors following the vaccination/infection to baseline as established by the negative donor group, the % frequencies and numbers of CD34+ cells per 1 mL of UCB against the days post-second vaccination were plotted (Figures 1C and 1D). Both parameters were inversely correlated with the term following the vaccination, though there was no significance difference by the positivity for IgGs against SARS-CoV-2 S and N proteins, indicating that these impacts on CD34+ cells were largely caused by the vaccination, in which the trends continued without recovering to baseline over the entire gestation period.

To understand the major cause of these impacts against CD34+ cells in the UCB, the levels of apoptosis in the CD34+ cell fractions from the double-positive groups with or without vaccination were assessed by Annexin-V staining using a gating strategy shown in Figure S5. Annexin-V positivity seemed to be higher in both infected groups irrespective of the vaccination compared to the negative group (Figure 2A). It is known that recombinant SARS-CoV-2 S proteins interfere with the viability and hematopoiesis of CD34+ cells when they are experimentally incubated ex vivo.[26,43] Thus, two independent assays were performed to confirm the presence of any free S proteins in the UCB plasma but were unsuccessful (Figures S6A and S6B). As other factors impact CD34+ cell fate, four major inflammatory cytokines (TNF-α, IFN-γ, IL-6, and IL-8) were quantified in the UCB plasma, all of which directly induce apoptosis and growth cessation of CD34+ cells as well as affect hematopoietic abilities of CD34+ cells.[44,45] Unfortunately, quantification was also unsuccessful even with using high/ultra-sensitive ELISA kits developed by Thermo Fisher Scientific (Figure S7, TNF-α and IFN-γ were undetectable). As a more comprehensive approach, transcriptomes from donor groups' CD34+ cells were compared to identify differentially expressed genes via total RNA sequencing analysis in the negative and double-positive groups (Figures 2B and 2C; N1-N4 versus DP1-DP4, respectively). The data revealed significant changes in expressions of 541 genes with log >2-fold changes, including 60-coding genes (20 increased and 40 decreased genes) between those groups. The gene ontology (GO) analysis revealed major significant changes were seen in genes related to IFN-γ-mediated signaling pathways, which includes HLA-class II genes, such as HLA-DQA1, HLA-DQB1, HLA-DRA, HLA-DRB1 and HLA-DRB5, suggesting that there is a change in the population of HSPCs.[46,47] Taken together, these data suggest that the IFN-γ-related signaling pathways promoted by SARS-CoV-2 infection could be involved in the induction of apoptosis observed in CD34+ HSPCs and thus might affect the fate and survivability of CD34+ HSPC populations in the UCB.

Previous SARS-CoV-2 infection skews the hematopoietic profile of CD34+ cells in UCB

The above results indicated that the frequency and total number of CD34+ cells in the UCB decreased in donors with previous SARS-CoV-2 infection and vaccination because of the induction of apoptosis, likely attributed by IFN-γ-mediated signaling pathways. Next, the hematopoietic ability of these CD34+ cells were assessed by two independent assays; an in vitro colony formation enabling evaluation of myeloid and erythroid lineages differentiation of each CD34+ cell,[48] and an in vivo hematopoietic differentiation by myeloablative xenotransplantation of human CD34+ HSPCs to immunodeficient neonatal mice (i.e., humanization) enabling evaluation of lymphoid as well as myeloid lineages differentiation.[48–50] Because of the poor recovery of CD34+ cells from the double positive donor groups after thawing cryopreserved stocks, these assays were only performed with negative and non-vaccinated N-/S+ donor groups' CD34+ cells. Although there was no major difference observed in the total colony formation unit (CFU) numbers between the groups, CD34+ cells from the N-/S+ group had significantly higher frequencies of burst-forming units erythroid (BFU-E) colonies as well as lower frequencies of granulocyte-erythrocyte-monocyte-megakaryocyte (CFU-GEMM) and granulocyte-macrophage (CFU-GM) colonies compared to the negative group (Figure 3B). The same CD34+ cells were further assessed with an in vivo hematopoiesis assay using two lines of immunodeficient mice, NSG and NSG-SGM3. Whole blood obtained from humanized NSG or NSG-SGM3 mice were analyzed using a gating strategy shown in Figure S8 with a definition of each leukocyte population indicated in Table S2. Although the NSG mouse strain enables reconstitution of lymphoid-lineage cells efficiently, the differentiation of myeloid lineage cells as well as NK cells is poor because of a lack of cytokines required for their reconstitutions. NSG-SGM3 mice, however, are transgenic to express three human cytokines, stem cell factor (SCF), granulocyte-macrophage colony-stimulating factor (GM-CSF), and IL-3, resulting in extensive support and thus differentiation of CD34+ cells to those
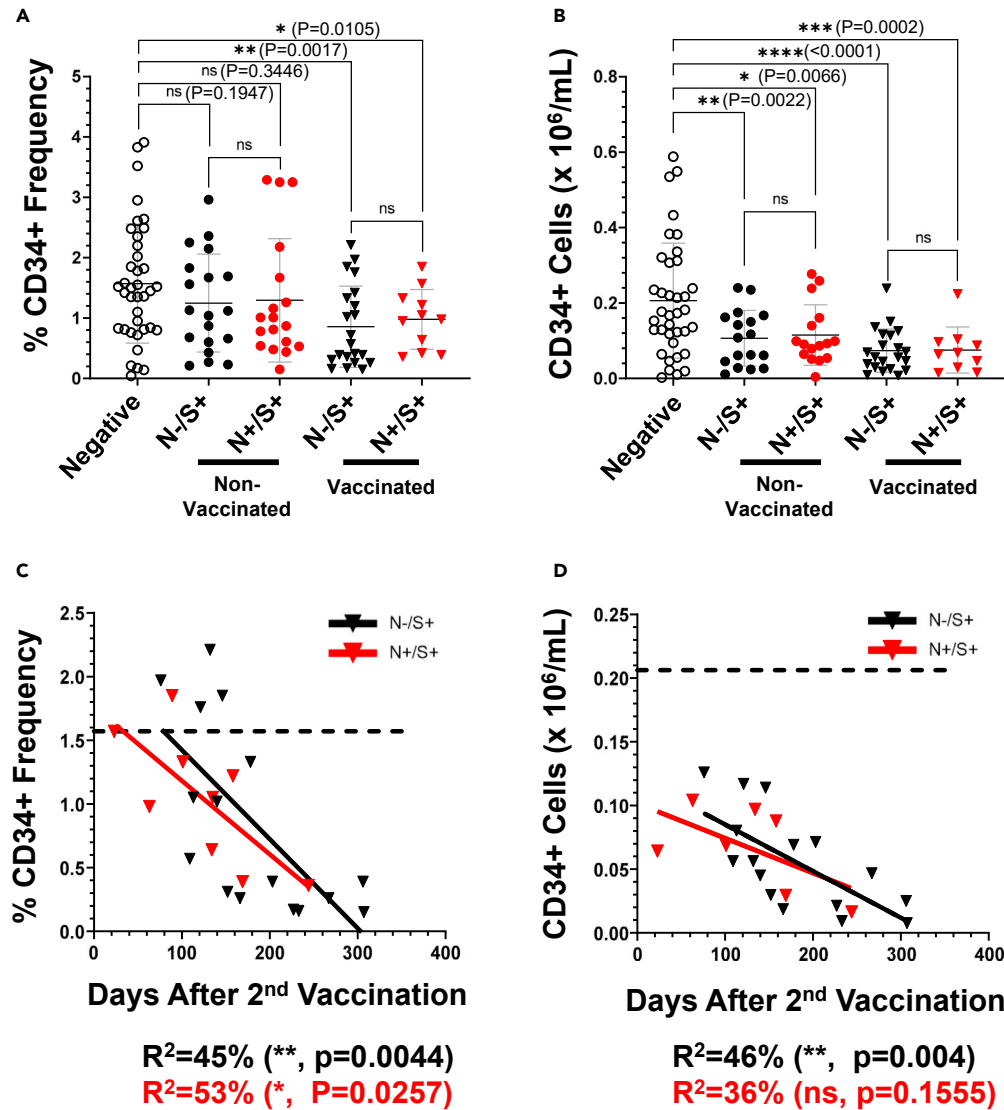
Figure 1. Previous SARS-CoV-2 infection and/or vaccination significantly decreases CD34+ cell frequencies and numbers per mL in UCB

(A and B) % Frequencies in MNC fractions (A) and total estimated numbers of CD34+ cells per mL of UCB (B) from each donor group. The CD34+ frequencies were obtained from flow cytometry by assessing the CD34+ population after doublet discrimination as in Figure S4. The total numbers per mL of UCB were calculated by multiplying the frequency of CD34+ cells in the MNCs by the MNC count for each donor and then dividing by the donor's UCB volume. A total 111 donor samples were analyzed for A and B (n = 39 for the negative, n = 21 and 19 for the N-/S+ and N+/S+ non-vaccinated groups, and n = 21 and 11 for the N-/S+ and N+/S+ vaccinated groups for C., respectively). Displayed are the means with standard deviation bars. p values of unpaired two-tailed t-test with Welch's correction and one-way ANOVA: ns (p>0.05), * (p<0.05), ** (p<0.005), *** (p<0.0005), **** (p<0.0001).

(C and D) Linear regression lines of the CD34+ cell frequencies in the MNC fraction versus days post-second SARS-CoV-2 vaccination (C), and the estimated CD34+ cell numbers per mL of UCB versus days post-second SARS-CoV-2 vaccination (D) The dashed line indicates the average CD34+ cell frequency in the MNC fraction (C) and the average CD34+ cell numbers per mL of UCB of the negative donor group as references (D), respectively. A total 25 donor samples were analyzed for C and D (n = 16 and 9 for N-/S+ and N+/S+ vaccinated groups). Data points colored black and red indicate donors single positive for anti-SARS-CoV-2 spike (S) protein IgG (N-/S+) and double-positive for both SARS-CoV-2 nucleocapsid (N) and S protein IgGs (N+/S+), respectively. Displayed are the R^2 values and the p values of non-zero slopes of the linear regression lines. p-values: ns (p>0.05), * (p<0.05), ** (p<0.005). Any values showing significance are shown.
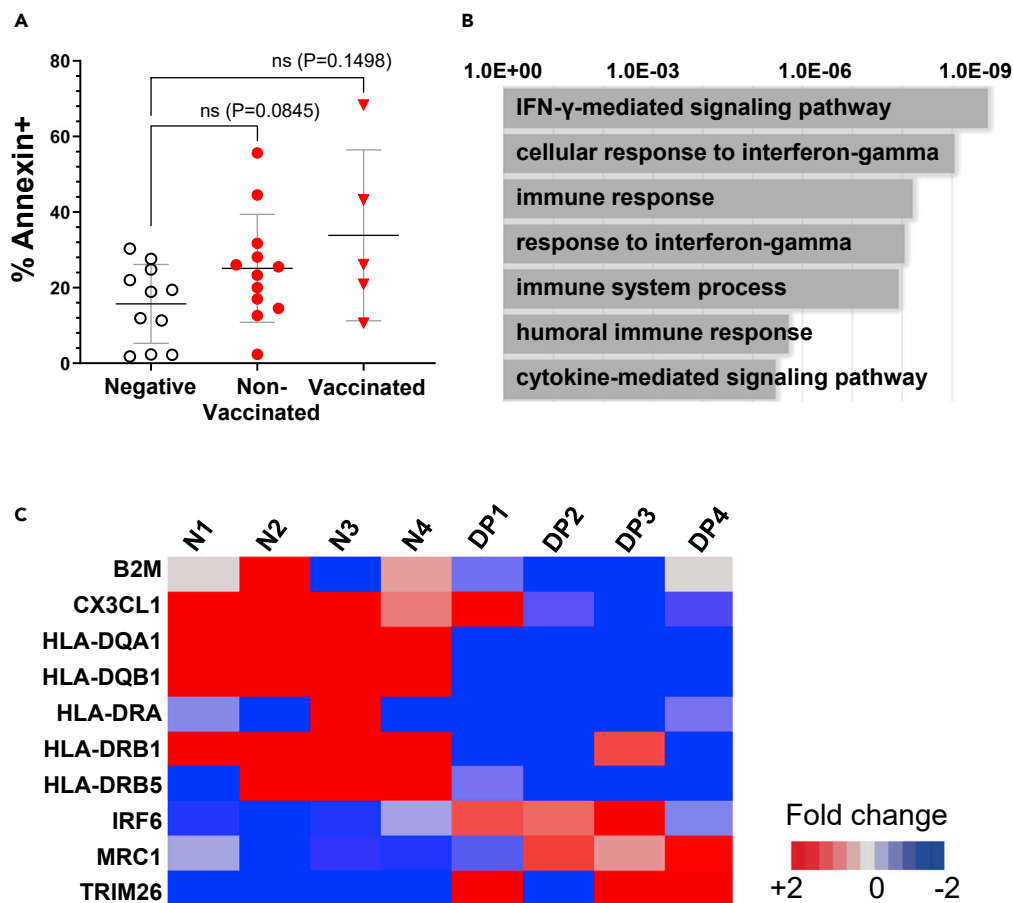
Figure 2. CD34+cells from donors with previous SARS-CoV-2 infection and vaccination are highly susceptible to apoptosis via IFN-γ-related pathways

(A) % Annexin-V positivity of CD34+ cell fractions. MNCs obtained from donors double-positive for anti-SARS-CoV-2 N and S protein IgGs (N+/S+) were used for CD34+ cell purification by autoMACS. 0.25 × 10^6 CD34+ cells (>98% purity) were used for staining with Biolegend PE Annexin-V and 7-AAD and analyzed by flow cytometry for apoptotic cells by Annexin-V+/7-AAD- as in Figure S5. Displayed are the means with standard deviation bars. p values of unpaired two-tailed t-test with Welch's correction: ns (p>0.05).

(B) Bar plot showing enrichment in different gene ontology (GO) terms predicted by GO analysis of top differentially expressed genes (p ≤ 0.05).

(C) Heatmap representing differentially expressed genes belonging to the "IFN-γ-mediated signaling pathway" and "Cellular response to IFN-γ" gene ontology terms significantly suppressed in CD34+ cells from the N+/S+ non-vaccinated donor group. N1-N4: samples from negative group (n = 4), DP1-DP4: samples from the N+/S+ non-vaccinated group (n = 4).

cells.[51,52] The blood of NSG mice reconstituted with CD34+ cells from the non-vaccinated N-/S+ group exhibited significantly higher frequencies of T cells, specifically CD8+T cells, yet lower B cell frequencies, which is represented by the higher T/B cell ratios, compared to the negative group (Figure 4A). Similar trends were also observed in the NSG-SGM3 mice humanized with CD34+ cells from the N-/S+ group, in addition to poor NK cell differentiation Figure 4B). The frequencies of total human lymphocytes as determined by flow cytometric analysis of the human CD45+ cell frequencies in the mouse blood were similar in both strains of mice, indicating that the CD34+ cells from donors with previous SARS-CoV-2 infection can support similar quantities and rates of hematopoiesis but exhibit altered frequencies and differentiation of HSPC populations.

DISCUSSION

The impact of SARS-CoV-2 infection and/or vaccination on CD34+ HSPCs in UCB has not been fully addressed nor studied at the cellular level. We here assessed potential damages of previous SARS-CoV-2
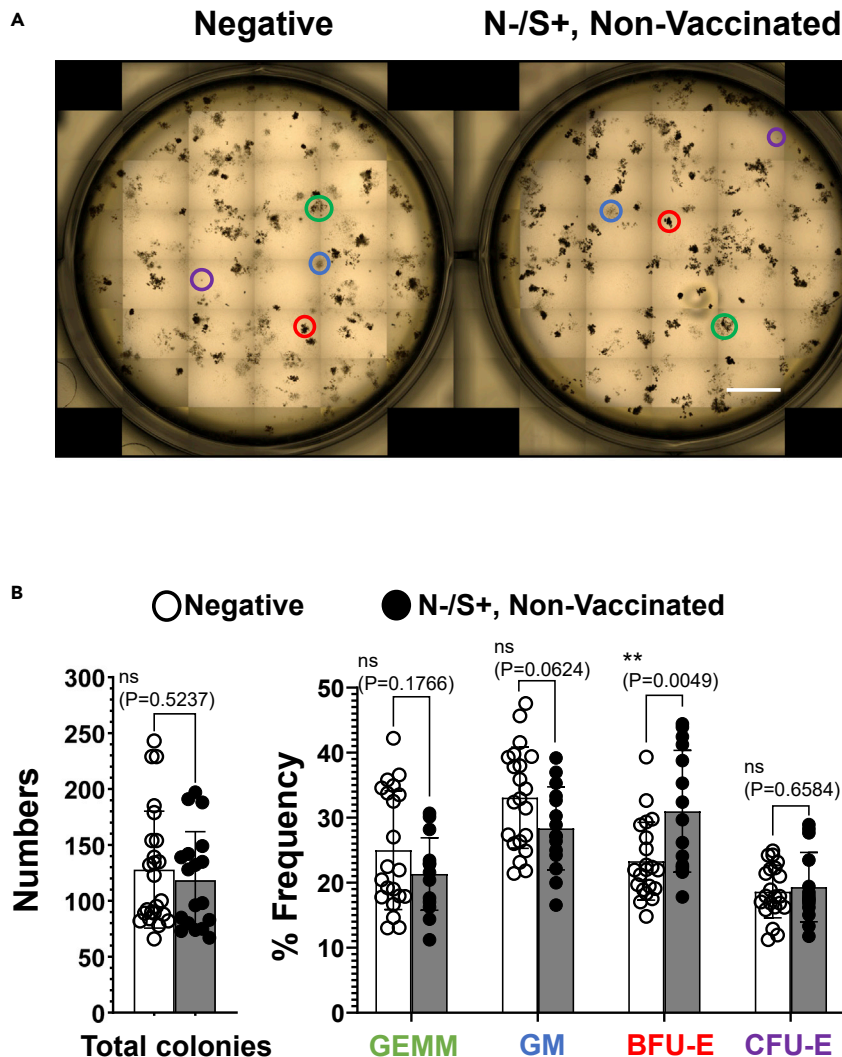
Figure 3. Hematopoietic differentiation *in vitro* is skewed by previous SARS-CoV-2 infection

(A) Representative images of the *in vitro* hematopoietic differentiation assay. Circled in the images are characteristic colony morphologies. Green: CFU-GEMM, Blue: CFU-GM, Red: BFU-E, Purple: CFU-E. Scale bar: 5 mm.

(B) Total colony numbers and % frequencies of CFU each lineage. 1×10^3 CD34$^+$ cells were used for the methylcellulose assay. After 14 days of incubation at 37°C, 5% CO_2, each 6-well plate was imaged by the EVOS M7000, and numbers of each colony type were manually counted as in A. Three experimental and biological replicates were performed per donor (n = 7 donors for each group). Displayed are the means with standard deviation bars. p values of unpaired two-tailed t-test with Welch's correction: ns (p>0.05), ** (p<0.005). CFU: colony formation units.

infection and/or vaccination on the fate and hematopoietic abilities of CD34$^+$ cells in the UCB thereof. Reduced CD34$^+$ cell frequencies and thus lower CD34$^+$ cell numbers were observed in the UCB from the non-vaccinated but previously infected donor group and even more so in the vaccinated donor group, which was attributed to the induction of apoptosis. Furthermore, these reductions in CD34$^+$ cell numbers and frequencies correlated with the timing of the second-vaccination in donors the numbers and frequencies inversely correlated with the period after the vaccination until delivery, indicating that factors causing these damages are maintained over the gestation period. In addition, the CD34$^+$ cells, which would be residual cells following apoptosis, showed skewed hematopoiesis profiles, indicating that previous SARS-CoV-2 infection, and likely vaccination based on the observed trends, interferes not only with the fate of CD34$^+$ cells but also the hematopoietic abilities, phenotype, and survivability of populations thereof, which could result in a shortage of available CD34$^+$ HSPCs from cord blood banking, processing for use toward HSPC-based therapies, as well as unpredictable hematological issues in HSPC recipients.
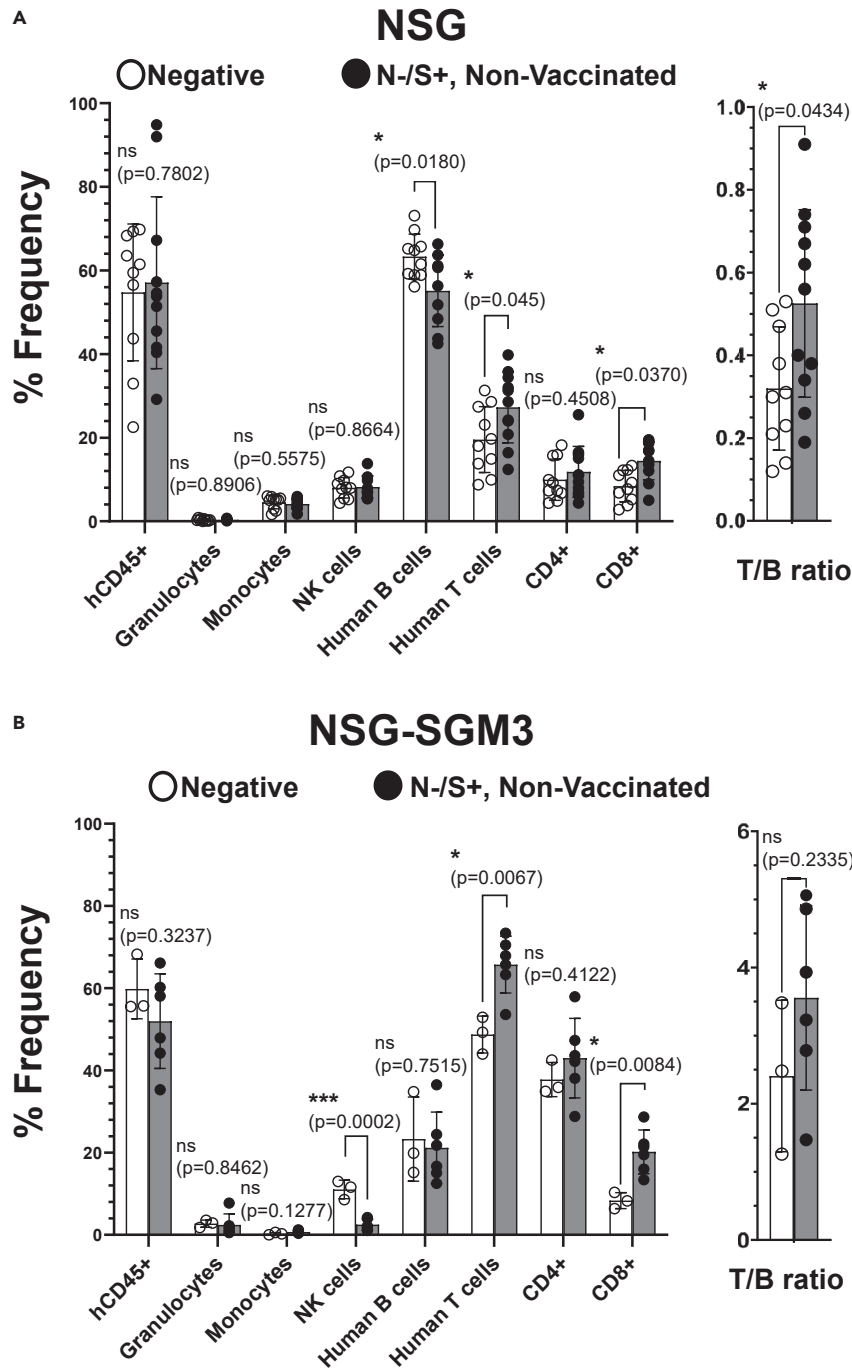
Figure 4. _In vivo_ hematopoiesis of CD34⁺ cells is skewed by previous SARS-CoV-2 infection

(A and B) X-ray irradiated (120 cGy) NSG (A) or NSG-SGM3 (B) neonate mice (days 1-3) were administered 0.1 × 10⁶ CD34⁺ cells via facial vein, which were obtained from 4 donors in the N-/S- (n = 10 NSG and n = 3 NSG-SGM3 mice) and N/-S+ non-vaccinated groups (n = 11 NSG and n = 6 NSG-SGM3 mice). Peripheral blood (100 μL) was obtained from the retro-orbital vein at 10 weeks post-humanization, stained with an antibody cocktail containing anti-human CD4, CD8, CD14, CD19, CD56, CD66b, CD45, and anti-mouse CD45 antibodies, and analyzed on FACSymphony. % Frequencies of each lineage of human blood cells were calculated as a percent of the total hCD45 and analyzed based on the positivity of the marker for each lineage as in Figure S8. % Frequencies of hCD45 was calculated as a percent frequency of the total human and mouse CD45⁺ population. T/B cell ratios were calculated by dividing the frequencies of the T/B cell populations. Displayed are the means with standard deviation bars. p values of unpaired two-tailed t-test with Welch's correction: ns (p>0.05), * (p<0.05), *** (p<0.0005). Markers used for defining each blood population were listed in Table S2.

Although it is not completely understood why UCB CD34$^+$ cells were becoming apoptotic, no or undetectable levels of free S proteins nor N antigens (data not shown) in the UCB plasma were observed, indicating that there were no or undetectable levels of SARS-CoV-2 viruses or free S proteins derived from the vaccine or the viral infection interfering with CD34$^+$ HSPCs' differentiation and survivability. In addition, there were no differences in levels of four residual inflammatory cytokines in the UCB plasma. The transcriptome assay suggested the involvement of IFN-γ-dependent signaling pathways as represented by changes in expressions of HLA-class II genes, in which expression is controlled by HLA-class II *trans* activator gene (CIITA). Importantly, IFN-γ is one of the key regulators for CIITA, and the increased level of IFN-γ mediates upregulation of CIITA, resulting in an upregulation of various HLA-class IIs.[53–55] As such, the differences in the expression level of HLA-class II in the UCB cells suggest the increased levels of IFN-γ in the past. Indeed, our transcriptome data indicated significant decreases of some HLA-class II expressions (HLA-DQA1, HLA-DQB1, HLA-DRA, HLA-DRB1, and HLA-DRB5) in purified CD34$^+$ cells from UCB donors in the N+/S+ non-vaccinated group. If the continuous IFN-γ stimulation was present in the donor, these levels should more increase.[53,54] Importantly, IFN-γ disrupts quiescence of HSPCs and promotes excessive terminal differentiation via bone marrow stromal cell antigen 2 (BST2) that mediates HSPC delocalization and activation.[25,56] Another report also indicated negative impacts of IFN-γ on HSPCs in terms of multilineage engraftment as well as self-renewability.[57] More recently, it has also been indicated that BNT162b2 mRNA COVID-19 vaccine significantly increases the levels of IFN-γ in the vaccinated subjects more than the infected subjects.[58–62] As such, one of the potential reasons for the decrease in UCB CD34$^+$ cells obtained from the N+/S+ donor groups would be continuous stimulation of them by IFN-γ over the course of gestation locally, such as in the feral liver, bone marrow, or the fetal spleen before circulating in the UCB.[63] The decrease and the stress-induced differentiation of CD34$^+$ HSPCs observed attributes to decreased circulating peripheral lymphocytes in fetuses, resulting in lower MNC numbers in the UCB. At present, it is unknown how these damages on CD34$^+$ cells are impactful to the neonate immune system for example, for fighting other pathogenic viruses, bacterial infections, or cancerous cells, as well as for maintaining homeostatic hematopoiesis, proper humoral and cellular immunities. These quantitative and qualitative changes in CD34$^+$ HSPCs of UCB might be impactful on the usage of these cells for therapeutic purposes. In addition, other major vaccines, such as influenza vaccines[64] or BCG[65] as well as bacterial pneumonia[66] also induce IFN-γ release, but their impacts on CD34$^+$ HSPCs are currently unknown. These vaccinations or the infection during the gestation period could be impactful on CD34$^+$ cells in UCB as well. The mouse humanization assay used in this manuscript can be a good tool for evaluating these potential concerns. In mouse humanization experiments, we have only studied levels of human blood cell reconstitution in peripheral blood. This is a limitation for deeper understanding of an impact of the infection or vaccination on CD34$^+$ HSPCs. Prolonged follow-up studies as well as additional studies, including human blood cell analysis in the bone marrow and lymphoid organs, would be required for better understanding of these impacts on them.

The limited numbers of CD34$^+$ cells in the UCB of the vaccinated donor groups were the greatest impediment, especially for the hematopoiesis differentiation assays, transcriptomics at the single cell level, as well as all statistical analyses. The use of freshly isolated MNCs for humanization following depletion of incoming T cells by anti-CD3 antibodies[67] or pre-expanding CD34$^+$ cells *ex vivo*[68,69] would be required to assess the impact of SARS-CoV-2 vaccination on UCB CD34$^+$ cells and hematopoiesis in future experiments. These studies should serve as a touchstone for understanding these potential impacts and provide insight about how the long-term side effects of SARS-CoV-2 infection and/or vaccination in mothers and even neonates affect future human immune health.

Limitations of the study

We used a humanized mouse model to evaluate hematopoietic ability of human CD34$^+$ cells. This model allows us to reconstitute human blood system under a mouse environment, but mice utilized for the assay do not support a complete human hematopoietic environment required for fully intact human blood cell reconstitution. This is one known caveat of the assay. Further detailed studies, such as a prolonged following up of blood phenotypes in donors delivered from mothers with SARS-CoV-2 infection or COVID-19 vaccination history over the course of patient growth, would be required to fully understand the impacts of the infection or the vaccination on their CD34$^+$ HSPCs.

STAR★METHODS

Detailed methods are provided in the online version of this paper and include the following:

- KEY RESOURCES TABLE

- RESOURCE AVAILABILITY
  - Lead contact
  - Materials availability
  - Data and code availability
- EXPERIMENTAL MODEL AND SUBJECTDETAILS
  - Human studies
  - *In vivo* animal studies
  - Cell lines
- METHOD DETAILS
  - Isolation of MNCs and CD34$^+$ cell fraction
  - Flow cytometry
  - Detection of SARS-CoV-2 spike proteins
  - Cytokine ELISAs
  - Detection of SARS-CoV2 S and N antibodies
  - *In vitro* and *in vivo* hematopoiesis assays
  - Transcriptome analysis
- QUANTIFICATION AND STATISTICAL ANALYSIS

AUTHOR CONTRIBUTIONS

B.K.E., C.J.K., and G.S. performed the experiments, analyzed data, and wrote the paper. S.O., Y.N.K., M.B., C.S., and C.E.J., performed the experiments. P.G., contributed to the study design. M.K., contributed to the study design, performed the experiments, interpreted data, and wrote the paper. All authors reviewed the manuscript.

DECLARATION OF INTERESTS

The authors declare no competing financial interests.

REFERENCES

1. Stefaniak, M., Dmoch-Gajzlerska, E., Mazurkiewicz, B., and Gajzlerska-Majewska, W. (2019). Maternal serum and cord blood leptin concentrations at delivery. PLoS One *14*, e0224863. https://doi.org/10.1371/journal.pone.0224863.

2. Unternaehrer, E., Bolten, M., Nast, I., Staehli, S., Meyer, A.H., Dempster, E., Hellhammer, D.H., Lieb, R., and Meinlschmidt, G. (2016). Maternal adversities during pregnancy and cord blood oxytocin receptor (OXTR) DNA methylation. Soc. Cogn. Affect. Neurosci. *11*, 1460–1470. https://doi.org/10.1093/scan/nsw051.

3. Hanion-Lundberg, K.M., Kirby, R.S., Gandhi, S., and Broekhuizen, F.F. (1997). Nucleated red blood cells in cord blood of singleton term neonates. Am. J. Obstet. Gynecol. *176*, 1149–1154. , discussion 1154-1156; discussion 1154-1146. https://doi.org/10.1016/s0002-9378(97)70328-70334.

4. Prabhu, S.B., Rathore, D.K., Nair, D., Chaudhary, A., Raza, S., Kanodia, P., Sopory, S., George, A., Rath, S., Bal, V., et al. (2016). Comparison of human neonatal and adult blood leukocyte subset composition phenotypes. PLoS One *11*, e0162242. https://doi.org/10.1371/journal.pone.0162242.

5. Carroll, D., and St Clair, D.K. (2018). Hematopoietic stem cells: normal versus malignant. Antioxid. Redox Signal. *29*, 1612–1632. https://doi.org/10.1089/ars.2017.7326.

6. Gurusamy, N., Alsayari, A., Rajasingh, S., and Rajasingh, J. (2018). Adult stem cells for regenerative therapy. Prog. Mol. Biol. Transl. Sci. *160*, 1–22. https://doi.org/10.1016/bs.pmbts.2018.07.009.

7. Lund, T.C. (2013). Hematopoietic stem cell transplant for lysosomal storage diseases. Pediatr. Endocrinol. Rev. *11*, 91–98.

8. Orchard, K., Dignan, F.L., Lee, J., Pearce, R., Desai, M., McFarlane, E., Parkin, A., Shearn, P., and Snowden, J.A. (2021). The NICE COVID-19 rapid guideline on haematopoietic stem cell transplantation: development, implementation and impact. Br. J. Haematol. *192*, 467–473. https://doi.org/10.1111/bjh.17280.

9. Pearson, T., Greiner, D.L., and Shultz, L.D. (2008). Creation of "humanized" mice to study human immunity. Curr Protoc Immunol. Curr. Protoc. Immunol. *Chapter 15*, Unit 15.21. https://doi.org/10.1002/0471142735.im1521s81.

10. Singh, S., Jakubison, B., and Keller, J.R. (2020). Protection of hematopoietic stem cells from stress-induced exhaustion and aging. Curr. Opin. Hematol. *27*, 225–231. https://doi.org/10.1097/MOH.0000000000000586.

11. Mitroulis, I., Kalafati, L., Bornhäuser, M., Hajishengallis, G., and Chavakis, T. (2020). Regulation of the bone marrow niche by inflammation. Front. Immunol. *11*, 1540. https://doi.org/10.3389/fimmu.2020.01540.

12. Andersen, K.G., Rambaut, A., Lipkin, W.I., Holmes, E.C., and Garry, R.F. (2020). The proximal origin of SARS-CoV-2. Nat. Med. *26*, 450–452. https://doi.org/10.1038/s41591-020-0820-9.

13. Zhou, P., Yang, X.L., Wang, X.G., Hu, B., Zhang, L., Zhang, W., Si, H.R., Zhu, Y., Li, B., Huang, C.L., et al. (2020). Addendum: a pneumonia outbreak associated with a new coronavirus of probable bat origin. Nature *588*, E6. https://doi.org/10.1038/s41586-020-2951-z.

14. Blomberg, B., Mohn, K.G.I., Brokstad, K.A., Zhou, F., Linchausen, D.W., Hansen, B.A., Lartey, S., Onyango, T.B., Kuwelker, K., Sævik, M., et al. (2021). Long COVID in a prospective cohort of home-isolated patients. Nat. Med. *27*, 1607–1613. https://doi.org/10.1038/s41591-021-01433-3.

15. Yan, Z., Yang, M., and Lai, C.L. (2021). Long COVID-19 syndrome: a comprehensive review of its effect on various organ systems and recommendation on rehabilitation plans. Biomedicines 9, 966. https://doi.org/10.3390/biomedicines9080966.

16. Bliddal, S., Banasik, K., Pedersen, O.B., Nissen, J., Cantwell, L., Schwinn, M., Tulstrup, M., Westergaard, D., Ullum, H., Brunak, S., et al. (2021). Acute and persistent symptoms in non-hospitalized PCR-confirmed COVID-19 patients. Sci. Rep. *11*, 13153. https://doi.org/10.1038/s41598-021-92045-x.

17. Pardi, N., Hogan, M.J., Porter, F.W., and Weissman, D. (2018). mRNA vaccines - a new era in vaccinology. Nat. Rev. Drug Discov. *17*, 261–279. https://doi.org/10.1038/nrd.2017.243.

18. Garcia-Flores, V., Romero, R., Xu, Y., Theis, K.R., Arenas-Hernandez, M., Miller, D., Peyvandipour, A., Bhatti, G., Galaz, J., Gershater, M., et al. (2022). Maternal-fetal immune responses in pregnant women infected with SARS-CoV-2. Nat. Commun. *13*, 320. https://doi.org/10.1038/s41467-021-27745-z.

19. Shimabukuro, T.T., Kim, S.Y., Myers, T.R., Moro, P.L., Oduyebo, T., Panagiotakopoulos, L., Marquez, P.L., Olson, C.K., Liu, R., Chang, K.T., et al. (2021). Preliminary findings of mRNA covid-19 vaccine safety in pregnant persons. N. Engl. J. Med. *384*, 2273–2282. https://doi.org/10.1056/NEJMoa2104983.

20. Golan, Y., Prahl, M., Cassidy, A.G., Gay, C., Wu, A.H.B., Jigmeddagva, U., Lin, C.Y., Gonzalez, V.J., Basilio, E., Warrier, L., et al. (2021). COVID-19 mRNA Vaccination in Lactation: Assessment of adverse effects and transfer of anti-SARS-CoV2 antibodies from mother to child. Preprint at medRxiv. https://doi.org/10.1101/2021.03.09.21253241.

21. Teijaro, J.R., and Farber, D.L. (2021). COVID-19 vaccines: modes of immune activation and future challenges. Nat. Rev. Immunol. *21*, 195–197. https://doi.org/10.1038/s41577-021-00526-x.

22. Perl, S.H., Uzan-Yulzari, A., Klainer, H., Asiskovich, L., Youngster, M., Rinott, E., and Youngster, I. (2021). SARS-CoV-2-Specific antibodies in breast milk after COVID-19 vaccination of breastfeeding women. JAMA *325*, 2013–2014. https://doi.org/10.1001/jama.2021.5782.

23. Trippella, G., Ciarcia, M., Ferrari, M., Buzzatti, C., Maccora, I., Azzari, C., Dani, C., Galli, L., and Chiappini, E. (2020). COVID-19 in pregnant women and neonates: a systematic review of the literature with quality assessment of the studies. Pathogens 9. https://doi.org/10.3390/pathogens9060485.

24. Prochaska, E., Jang, M., and Burd, I. (2020). COVID-19 in pregnancy: placental and neonatal involvement. Am. J. Reprod. Immunol. *84*, e13306. https://doi.org/10.1111/aji.13306.

25. King, K.Y., and Goodell, M.A. (2011). Inflammatory modulation of HSCs: viewing the HSC as a foundation for the immune response. Nat. Rev. Immunol. *11*, 685–692. https://doi.org/10.1038/nri3062.

26. Ropa, J., Cooper, S., Capitano, M.L., Van't Hof, W., and Broxmeyer, H.E. (2021). Human hematopoietic stem, progenitor, and immune cells respond ex vivo to SARS-CoV-2 spike protein. Stem Cell Rev. Rep. *17*, 253–265. https://doi.org/10.1007/s12015-020-10056-z.

27. Wang, X., Wen, Y., Xie, X., Liu, Y., Tan, X., Cai, Q., Zhang, Y., Cheng, L., Xu, G., Zhang, S., et al. (2021). Dysregulated hematopoiesis in bone marrow marks severe COVID-19. Cell Discov. *7*, 60. https://doi.org/10.1038/s41421-021-00296-9.

28. Oltean, I., Tran, J., Lawrence, S., Ruschkowski, B.A., Zeng, N., Bardwell, C., Nasr, Y., de Nanassy, J., and El Demellawy, D. (2021). Impact of SARS-CoV-2 on the clinical outcomes and placental pathology of pregnant women and their infants: a systematic review. Heliyon 7, e06393. https://doi.org/10.1016/j.heliyon.2021.e06393.

29. Marinho, P.S., da Cunha, A.J.L.A., Chimelli, L., Avvad-Portari, E., Andreiuolo, F.D.M., de Oliveira-Szejnfeld, P.S., Mendes, M.A., Gomes, I.C., Souza, L.R.Q., Guimarães, M.Z., et al. (2021). Case report: SARS-CoV-2 mother-to-child transmission and fetal death associated with severe placental thromboembolism. Front. Med. *8*, 677001. https://doi.org/10.3389/fmed.2021.677001.

30. Alipour, Z., Samadi, P., Eskandari, N., Ghaedrahmati, M., Vahedian, M., Khalajinia, Z., and Mastanijahroodi, A. (2021). Relationship between coronavirus disease 2019 in pregnancy and maternal and fetal outcomes: retrospective analytical cohort study. Midwifery *102*, 103128. https://doi.org/10.1016/j.midw.2021.103128.

31. Karasek, D., Baer, R.J., McLemore, M.R., Bell, A.J., Blebu, B.E., Casey, J.A., Coleman-Phox, K., Costello, J.M., Felder, J.N., Flowers, E., et al. (2021). The association of COVID-19 infection in pregnancy with preterm birth: a retrospective cohort study in California. Lancet Reg. Health. Am. *2*, 100027. https://doi.org/10.1016/j.lana.2021.100027.

32. Martinez-Perez, O., Prats Rodriguez, P., Muner Hernandez, M., Encinas Pardilla, M.B., Perez Perez, N., Vila Hernandez, M.R., Villalba Yarza, A., Nieto Velasco, O., Del Barrio Fernandez, P.G., Forcen Acebal, L., et al. (2021). The association between SARS-CoV-2 infection and preterm delivery: a prospective study with a multivariable analysis. BMC Pregnancy Childbirth 21, 273. https://doi.org/10.1186/s12884-021-03742-4.

33. Metz, T.D., Clifton, R.G., Hughes, B.L., Sandoval, G.J., Grobman, W.A., Saade, G.R., Manuck, T.A., Longo, M., Sowles, A., Clark, K., et al. (2022). Association of SARS-CoV-2 infection with serious maternal morbidity and mortality from obstetric complications. JAMA *327*, 748–759. https://doi.org/10.1001/jama.2022.1190.

34. Piekos, S.N., Roper, R.T., Hwang, Y.M., Sorensen, T., Price, N.D., Hood, L., and Hadlock, J.J. (2022). The effect of maternal SARS-CoV-2 infection timing on birth outcomes: a retrospective multicentre cohort study. Lancet. Digit. Health 4, e95–e104. https://doi.org/10.1016/S2589-7500(21)00250-8.

35. Bordt, E.A., Shook, L.L., Atyeo, C., Pullen, K.M., De Guzman, R.M., Meinsohn, M.C., Chauvin, M., Fischinger, S., Yockey, L.J., James, K., et al. (2021). Maternal SARS-CoV-2 infection elicits sexually dimorphic placental immune responses. Sci. Transl. Med. *13*, eabi7428. https://doi.org/10.1126/scitranslmed.abi7428.

36. Conti, M.G., Terreri, S., Terrin, G., Natale, F., Pietrasanta, C., Salvatori, G., Brunelli, R., Midulla, F., Papaevangelou, V., Carsetti, R., and Angelidou, A. (2022). SARS-CoV-2 infection versus vaccination in pregnancy: implications for maternal and infant immunity. Clin. Infect. Dis. 75, S37–S45. https://doi.org/10.1093/cid/ciac359.

37. Villar, J., Ariff, S., Gunier, R.B., Thiruvengadam, R., Rauch, S., Kholin, A., Roggero, P., Prefumo, F., do Vale, M.S., Cardona-Perez, J.A., et al. (2021). Maternal and neonatal morbidity and mortality among pregnant women with and without COVID-19 infection: the INTERCOVID multinational cohort study. JAMA Pediatr. 175, 817–826. https://doi.org/10.1001/jamapediatrics.2021.1050.

38. Ballen, K.K., Wilson, M., Wuu, J., Ceredona, A.M., Hsieh, C., Stewart, F.M., Popovsky, M.A., and Quesenberry, P.J. (2001). Bigger is better: maternal and neonatal predictors of hematopoietic potential of umbilical cord blood units. Bone Marrow Transplant. 27, 7–14. https://doi.org/10.1038/sj.bmt.1702729.

39. Nunes, R.D., and Zandavalli, F.M. (2015). Association between maternal and fetal factors and quality of cord blood as a source of stem cells. Rev. Bras. Hematol. Hemoter. 37, 38–42. https://doi.org/10.1016/j.bjhh.2014.07.023.

40. Sah, P., Fitzpatrick, M.C., Zimmer, C.F., Abdollahi, E., Juden-Kelly, L., Moghadas, S.M., Singer, B.H., and Galvani, A.P. (2021). Asymptomatic SARS-CoV-2 infection: a systematic review and meta-analysis. Proc. Natl. Acad. Sci. USA 118. e2109229118. https://doi.org/10.1073/pnas.2109229118.

41. Wei, J., Matthews, P.C., Stoesser, N., Maddox, T., Lorenzi, L., Studley, R., Bell, J.I., Newton, J.N., Farrar, J., Diamond, I., et al. (2021). Anti-spike antibody response to natural SARS-CoV-2 infection in the general population. Nat. Commun. 12, 6250. https://doi.org/10.1038/s41467-021-26479-2.

42. Lumley, S.F., Wei, J., O'Donnell, D., Stoesser, N.E., Matthews, P.C., Howarth, A., Hatch, S.B., Marsden, B.D., Cox, S., James, T., et al. (2021). The duration, dynamics, and determinants of severe acute respiratory syndrome coronavirus 2 (SARS-CoV-2) antibody responses in individual Healthcare workers. Clin. Infect. Dis. 73, e699–e709. https://doi.org/10.1093/cid/ciab004.

43. Kucia, M., Ratajczak, J., Bujko, K., Adamiak, M., Ciechanowicz, A., Chumak, V., Brzezniakiewicz-Janus, K., and Ratajczak, M.Z. (2021). An evidence that SARS-Cov-2/COVID-19 spike protein (SP) damages hematopoietic stem/progenitor cells in the mechanism of pyroptosis in Nlrp3 inflammasome-dependent manner. Leukemia 35, 3026–3029. https://doi.org/10.1038/s41375-021-01332-z.

44. Caiado, F., Pietras, E.M., and Manz, M.G. (2021). Inflammation as a regulator of hematopoietic stem cell function in disease, aging, and clonal selection. J. Exp. Med. 218, e20201541. https://doi.org/10.1084/jem.20201541.

45. Gogoleva, V.S., Atretkhany, K.S.N., Dygay, A.P., Yurakova, T.R., Drutskaya, M.S., and Nedospasov, S.A. (2021). Current perspectives on the role of TNF in hematopoiesis using mice with humanization of TNF/LT system. Front. Immunol. 12, 661900. https://doi.org/10.3389/fimmu.2021.661900.

46. Finkielsztein, A., Schlinker, A.C., Zhang, L., Miller, W.M., and Datta, S.K. (2015). Human megakaryocyte progenitors derived from hematopoietic stem cells of normal individuals are MHC class II-expressing professional APC that enhance Th17 and Th1/Th17 responses. Immunol. Lett. 163, 84–95. https://doi.org/10.1016/j.imlet.2014.11.013.

47. Falkenburg, J.H., Fibbe, W.E., Goselink, H.M., Van Rood, J.J., and Jansen, J. (1985). Human hematopoietic progenitor cells in long-term cultures express HLA-DR antigens and lack HLA-DQ antigens. J. Exp. Med. 162, 1359–1369. https://doi.org/10.1084/jem.162.4.1359.

48. Ringpis, G.E.E., Shimizu, S., Arokium, H., Camba-Colón, J., Carroll, M.V., Cortado, R., Xie, Y., Kim, P.Y., Sahakyan, A., Lowe, E.L., et al. (2012). Engineering HIV-1-resistant T-cells from short-hairpin RNA-expressing hematopoietic stem/progenitor cells in humanized BLT mice. PLoS One 7, e53492. https://doi.org/10.1371/journal.pone.0053492.

49. Wen, J., Wang, L., Ren, J., Kranz, E., Chen, S., Wu, D., Kanazawa, T., Chen, I., Lu, Y., and Kamata, M. (2021). Nanoencapsulated rituximab mediates superior cellular immunity against metastatic B-cell lymphoma in a complement competent humanized mouse model. J. Immunother. Cancer 9, e001524. https://doi.org/10.1136/jitc-2020-001524.

50. Zhen, A., Rezek, V., Youn, C., Rick, J., Lam, B., Chang, N., Zack, J., Kamata, M., and Kitchen, S. (2016). Stem-cell based engineered immunity against HIV infection in the humanized mouse model. J. Vis. Exp. https://doi.org/10.3791/54048.

51. Zhang, Z., Guo, L., Lu, X., Zhang, C., Huang, L., Wang, X., Duan, F., Liang, H., Chen, P., Zeng, L., et al. (2021). Clinical analysis and pluripotent stem cells-based model reveal possible impacts of ACE2 and lung progenitor cells on infants vulnerable to COVID-19. Theranostics 11, 2170–2181. https://doi.org/10.7150/thno.53136.

52. Zauche, L.H., Wallace, B., Smoots, A.N., Olson, C.K., Oduyebo, T., Kim, S.Y., Peterson, E.E., Ju, J., Beauregard, J., Wilcox, A.J., et al. (2021). Receipt of mRNA COVID-19 vaccines preconception and during pregnancy and risk of self-reported spontaneous abortions, CDC V-Safe COVID-19 vaccine pregnancy registry 2020-21. Res. Sq. https://doi.org/10.21203/rs.3.rs-798175/v1.

53. Keskinen, P., Ronni, T., Matikainen, S., Lehtonen, A., and Julkunen, I. (1997). Regulation of HLA class I and II expression by interferons and influenza A virus in human peripheral blood mononuclear cells. Immunology 91, 421–429. https://doi.org/10.1046/j.1365-2567.1997.00258.x.

54. Steimle, V., Siegrist, C.A., Mottet, A., Lisowska-Grospierre, B., and Mach, B. (1994). Regulation of MHC class II expression by interferon-gamma mediated by the transactivator gene CIITA. Science 265, 106–109. https://doi.org/10.1126/science.8016643.

55. Croce, M., De Ambrosis, A., Corrias, M.V., Pistoia, V., Occhino, M., Meazza, R., Giron-Michel, J., Azzarone, B., Accolla, R.S., and Ferrini, S. (2003). Different levels of control prevent interferon-gamma-inducible HLA-class II expression in human neuroblastoma cells. Oncogene 22, 7848–7857. https://doi.org/10.1038/sj.onc.1207054.

56. Florez, M.A., Matatall, K.A., Jeong, Y., Ortinau, L., Shafer, P.W., Lynch, A.M., Jaksik, R., Kimmel, M., Park, D., and King, K.Y. (2020). Interferon gamma mediates hematopoietic stem cell activation and niche relocalization through BST2. Cell Rep. 33, 108530. https://doi.org/10.1016/j.celrep.2020.108530.

57. Yang, L., Dybedal, I., Bryder, D., Nilsson, L., Sitnicka, E., Sasaki, Y., and Jacobsen, S.E.W. (2005). IFN-gamma negatively modulates self-renewal of repopulating human hemopoietic stem cells. J. Immunol. 174, 752–757. https://doi.org/10.4049/jimmunol.174.2.752.

58. Herzberg, J., Fischer, B., Lindenkamp, C., Becher, H., Becker, A.K., Honarpisheh, H., Guraya, S.Y., Strate, T., and Knabbe, C. (2022). Persistence of immune response in health care workers after two doses BNT162b2 in a longitudinal observational study. Front. Immunol. 13, 839922. https://doi.org/10.3389/fimmu.2022.839922.

59. Sahin, U., Muik, A., Derhovanessian, E., Vogler, I., Kranz, L.M., Vormehr, M., Baum, A., Pascal, K., Quandt, J., Maurus, D., et al. (2020). COVID-19 vaccine BNT162b1 elicits human antibody and TH1 T cell responses. Nature 586, 594–599. https://doi.org/10.1038/s41586-020-2814-7.

60. Tober-Lau, P., Schwarz, T., Vanshylla, K., Hillus, D., Gruell, H., EICOV/COVIM Study Group, Suttorp, N., Landgraf, I., Kappert, K., Seybold, J., et al. (2021). Long-term immunogenicity of BNT162b2 vaccination in older people and younger health-care workers. Lancet Respir. Med. 9, e104–e105. https://doi.org/10.1016/S2213-2600(21)00456-2.

61. Kurteva, E., Vasilev, G., Tumangelova-Yuzeir, K., Ivanova, I., Ivanova-Todorova, E., Velikova, T., and Kyurkchiev, D. (2022). Interferon-gamma release assays outcomes in healthy subjects following BNT162b2 mRNA COVID-19 vaccination. Rheumatol. Int. 42, 449–456. https://doi.org/10.1007/s00296-022-05091-7.

62. Barreiro, P., Sanz, J.C., San Román, J., Pérez-Abeledo, M., Carretero, M., Megías, G., Viñuela-Prieto, J.M., Ramos, B., Canora, J., Martínez-Peromingo, F.J., et al. (2022). A pilot study for the evaluation of an interferon gamma release assay (IGRA) to measure T-cell immune responses after SARS-CoV-2 infection or vaccination in a unique cloistered cohort. J. Clin. Microbiol. 60, e0219921. https://doi.org/10.1128/jcm.02199-21.

63. Lewis, K., Yoshimoto, M., and Takebe, T. (2021). Fetal liver hematopoiesis: from development to delivery. Stem Cell Res. Ther. *12*, 139. https://doi.org/10.1186/s13287-021-02189-w.

64. Athale, S., Banchereau, R., Thompson-Snipes, L., Wang, Y., Palucka, K., Pascual, V., and Banchereau, J. (2017). Influenza vaccines differentially regulate the interferon response in human dendritic cell subsets. Sci. Transl. Med. *9*, eaaf9194. https://doi.org/10.1126/scitranslmed.aaf9194.

65. Black, G.F., Weir, R.E., Floyd, S., Bliss, L., Warndorff, D.K., Crampin, A.C., Ngwira, B., Sichali, L., Nazareth, B., Blackwell, J.M., et al. (2002). BCG-induced increase in interferon-gamma response to mycobacterial antigens and efficacy of BCG vaccination in Malawi and the UK: two randomised controlled studies. Lancet *359*, 1393–1401. https://doi.org/10.1016/S0140-6736(02)08353-8.

66. Gomez, J.C., Yamada, M., Martin, J.R., Dang, H., Brickey, W.J., Bergmeier, W., Dinauer, M.C., and Doerschuk, C.M. (2015). Mechanisms of interferon-gamma production by neutrophils and its function during Streptococcus pneumoniae pneumonia. Am. J. Respir. Cell Mol. Biol. *52*, 349–364. https://doi.org/10.1165/rcmb.2013-0316OC.

67. Wunderlich, M., Brooks, R.A., Panchal, R., Rhyasen, G.W., Danet-Desnoyers, G., and Mulloy, J.C. (2014). OKT3 prevents xenogeneic GVHD and allows reliable xenograft initiation from unfractionated human hematopoietic tissues. Blood *123*, e134–e144. https://doi.org/10.1182/blood-2014-02-556340.

68. Yadav, P., Vats, R., Bano, A., and Bhardwaj, R. (2020). Hematopoietic stem cells culture, expansion and differentiation: an insight into variable and available media. Int. J. Stem Cells *13*, 326–334. https://doi.org/10.15283/ijsc19157.

69. Ghafouri-Fard, S., Niazi, V., Taheri, M., and Basiri, A. (2021). Effect of small molecule on ex vivo expansion of cord blood hematopoietic stem cells: aconcise review. Front. Cell Dev. Biol. *9*, 649115. https://doi.org/10.3389/fcell.2021.649115.

70. Jaatinen, T., and Laine, J. (2007). Isolation of mononuclear cells from human cord blood by Ficoll-Paque density gradient. Curr Protoc Stem Cell Biol. Curr. Protoc. Stem Cell Biol. *Chapter 2*, Unit 2A.1. https://doi.org/10.1002/9780470151808.sc02a01s1.

71. Wen, J., Wu, D., Qin, M., Liu, C., Wang, L., Xu, D., Vinters, H.V., Liu, Y., Kranz, E., Guan, X., et al. (2019). Sustained delivery and molecular targeting of a therapeutic monoclonal antibody to metastases in the central nervous system of mice. Nat. Biomed. Eng. *3*, 706–716. https://doi.org/10.1038/s41551-019-0434-z.

72. Qin, M., Wang, L., Wu, D., Williams, C.K., Xu, D., Kranz, E., Guo, Q., Guan, J., Vinters, H.V., Lee, Y., et al. (2019). Enhanced delivery of rituximab into brain and lymph nodes using timed-release nanocapsules in non-human primates. Front. Immunol. *10*, 3132. https://doi.org/10.3389/fimmu.2019.03132.

73. Khamaikawin, W., Shimizu, S., Kamata, M., Cortado, R., Jung, Y., Lam, J., Wen, J., Kim, P., Xie, Y., Kim, S., et al. (2018). Modeling anti-HIV-1 HSPC-based gene therapy in humanized mice previously infected with HIV-1. Mol. Ther. Methods Clin. Dev. *9*, 23–32. https://doi.org/10.1016/j.omtm.2017.11.008.

74. Dobin, A., Davis, C.A., Schlesinger, F., Drenkow, J., Zaleski, C., Jha, S., Batut, P., Chaisson, M., and Gingeras, T.R. (2013). STAR: ultrafast universal RNA-seq aligner. Bioinformatics *29*, 15–21. https://doi.org/10.1093/bioinformatics/bts635.

75. Anders, S., Pyl, P.T., and Huber, W. (2015). HTSeq–a Python framework to work with high-throughput sequencing data. Bioinformatics *31*, 166–169. https://doi.org/10.1093/bioinformatics/btu638.

76. Huang, D.W., Sherman, B.T., and Lempicki, R.A. (2009). Systematic and integrative analysis of large gene lists using DAVID bioinformatics resources. Nat. Protoc. *4*, 44–57. https://doi.org/10.1038/nprot.2008.211.

STAR★METHODS

KEY RESOURCES TABLE

REAGENT or RESOURCE	SOURCE	IDENTIFIER
Antibodies		
APC anti-human CD66b	BioLegend	CAT# 396906; clone QA17A51
PE/Cyanine7 anti-human CD3	BioLegend	CAT# 344816; clone SK7
Brilliant Violet (BV) 421 anti-human CD56	BioLegend	CAT# 362552; clone 5.1H11
BV510 anti-human CD4	BioLegend	CAT# 357420; clone A161A1
BV605 anti-human CD8	BioLegend	CAT# 344742; clone SK1
BV711 anti-human CD19	BioLegend	CAT# 302246; clone HIB19
BV785 anti-human CD14	BioLegend	CAT# 301840; clone M5E2
FITC anti-human CD45	BioLegend	CAT# 982316; clone HI30
PE anti-human CD34	BioLegend	CAT# 343506; clone 581
APC/Fire750 anti-mouse CD45	BioLegend	CAT# 147714; clone I3/2.3
PE-Annexin-V; 7-AAD apoptosis kit	BioLegend	CAT# 640934
Polyclonal Anti-SARS-Related Coronavirus 2 Spike Glycoprotein	BEI resources, VA	CAT# NR-52947
HRP-conjugated anti-rabbit IgG antibody	R&D, MN	CAT# HAF008
Chemicals, peptides, and recombinant proteins		
CD34 beads	Miltenyi Biotec, Germany	CAT# 130-046-703
RBC Fix & Lysis	BioLegend	CAT# 422401
Precision Count beads	BioLegend	CAT# 424902
Tween20	ThermoFisher Scientific, MA	CAT# J20605AP; CAS: 9005-64-5
Pierce™ ECL Plus Western Blotting Substrate	ThermoFisher Scientific	CAT# A38554
Protein A/G Magnetic Beads	MedChem Express, NJ	CAT# HY-K0202-5 mL
CHAPS	Millipore Sigma	CAT# 3055100GM; CAS: 75621-03-3
0.4% trypan blue	ThermoFisher	CAT# 15250061
Protein ladder for western blot	ThermoFisher Scientific	CAT# PI26619
Recombinant stabilized SARS-CoV-2 S protein	BEI resources	CAT# NR-55438
Polyvinylpyrrolidone	Millipore Sigma, MA	CAS No. 9003-39-8
Critical commercial assays		
IL-6 Human ELISA KIT	ThermoFischer Scientific	CAT# BMS213HS
IL-8 Human ELISA Kit	ThermoFischer Scientific	CAT# KHC0084
TNF-α Human ELISA Kit	ThermoFischer Scientific	CAT# BMS223HS
IFN-γ Human Uncoated ELISA kit	ThermoFischer Scientific	CAT# 88-7316-88
LEGEND MAX™ SARS-CoV-2 Nucleocapsid Human IgG ELISA Kit	BioLegend	CAT# 448107
SARS-CoV-2 IgG/IgM rapid antibody tests	AssureTech, MD	N/A
Quick-RNA kits	Zymo Research, CA	CAT# R1054
eStart Rapid COVID-19 antigen test	Intrivo, CA	CAT# RCHM-02071
Deposited data		
RNA sequencing data	GEO	accession number GEO: GSE196802
human reference genome	Gencode	GRCh38 p13, Release 36
Experimental models: Cell lines		
MethoCult H4434 Classic Methylcellulose Medium	StemCell Technologies, Canada	CAT# H4434

(Continued on next page)

Continued

REAGENT or RESOURCE	SOURCE	IDENTIFIER
Experimental models: Organisms/strains		
NOD.Cg-*Prkdc^scid Il2rg^tm1Wjl*/SzJ (NSG)	The Jackson Laboratory	Stock# 005557
NOD.Cg-*Prkdc^scid Il2rg^tm1Wjl* Tg (CMV-IL3, CSF2, KITLG)1Eav/MloySzJ (NSG-SGM3)	The Jackson Laboratory	Stock# 013062
Software and algorithms		
ImageJ	NIH	https://imagej.nih.gov/ij/
STAR, v2.7.7a	Alexander Dobin	https://anaconda.org/bioconda/star/files
HTSeq-count, v0.13.5	https://doi.org/10.1093/bioinformatics/btu638	https://pypi.org/project/HTSeq/
DESeq2	Bioconductor	https://bioconductor.org/packages/release/bioc/html/DESeq2.html
GraphPad Prism 9	Dotmatics	https://www.graphpad.com/scientific-software/prism/
DAVID Bioinformatics Resources	Laboratory of Human Retrovirology and Immunoinformatics (LHRI)	https://david.ncifcrf.gov/
Other		
sterile cord blood collection unit	MacoPharma, GA	CAT# MSC127D
autoMACS ProCell Separator	Miltenyi Biotec	N/A
BD FACSymphony	BD medical device, NJ	N/A
Precast Gel 4–12%	Nacalai USA, CA	CAT# NU041215
Typhoon Trio + Variable Mode Imager	GE Healthcare, GA	N/A
magnetic rack	Invitrogen, MA	N/A
EVOS M7000 imaging system	ThermoFisher Scientific, MA	N/A
Illumina NextSeq 500	Illumina, CA	N/A
Results and analyzed data	This paper	Request lead contact for data and help with analyses

RESOURCE AVAILABILITY

Lead contact

Further information and requests for resources, protocols, and reagents should be directed to and will be fulfilled by the lead contact, Masakazu Kamata (masa3k@uab.edu).

Materials availability

This study did not generate new unique reagents.

Data and code availability

- Data: All data reported in this paper will be shared by the lead contact upon request. RNA sequencing data are available at GEO: GSE196802 as of the date of the publication. Accession Numbers are also listed in the key resources table. All raw images, such as the microscopy of the hematopoiesis assay and the Western Blot images, will be shared by the lead contact upon request.
- Code: This paper does not report original code.
- Availability Statement: Any additional information required to reanalyze the data reported in this paper is available from the lead contact upon request.

EXPERIMENTAL MODEL AND SUBJECTDETAILS

Human studies

All human umbilical cord blood (UCB) samples were collected from females following vaginal delivery at University of Alabama at Birmingham Hospital giving written informed consent under an approved IRB

protocol (IRB-300004736). To exclude potential factors affecting UCB characteristics, the eligible donor population was selected for women who delivered vaginally after 37 weeks with babies weighing >2,500 g between March 18th, 2021, and December 15th, 2021. All enrolled donors with medical records indicating previous or active SARS-CoV-2 infection as determined by COVID-19 PCR assays or SARS-CoV-2 nucleocapsid (N) and/or Spike (S) antigens/proteins in the UCB and validated by the CareStart Rapid COVID-19 antigen test (Intrivo, CA) were excluded from the study. Previous asymptomatic infection of donors was determined by the presence of IgGs against SARS-CoV-2 nucleocapsid (N) and Spike (S) protein in the UCB plasma as determined by LEGEND MAX SARS-CoV-2 Nucleocapsid Human IgG ELISA Kit (BioLegend) and SARS-CoV-2 IgG/IgM rapid antibody tests (AssureTech, MD), respectively. Donors also tested negative for infection by HIV, HBV, and HCV (data not shown). A total of 111 donor samples were served for the assays and divided into 3 groups, including 5 subcategories: double-negative for anti-N and anti-S IgGs (N-/S- negative), non-vaccinated group positive for anti-S IgG (N-/S+, non-vaccinated) or both anti-N and anti-S IgGs (N+/S+, non-vaccinated), and the documented vaccinated group positive for anti-S IgG (N-/S+, vaccinated) or both anti-N and anti-S IgGs (N+/S+, vaccinated). Vaccinated donors received Pfizer's BNT162b2 (n = 24/32) or Moderna's mRNA-1273 (n = 8/32) vaccines. Ave. Average. Additional key information for donor group sample sizes and characteristics are listed in Table S1.

In vivo animal studies

The in vivo hematopoiesis assay was performed by humanization of two immunodeficient mouse strains: NOD.Cg-$Prkdc^{scid}$ $Il2rg^{tm1Wjl}$/SzJ (NSG) and NOD.Cg-$Prkdc^{scid}$ $Il2rg^{tm1Wjl}$ Tg (CMV-IL3, CSF2, KITLG) 1Eav/MloySzJ (NSG-SGM3). For preparation of the mice at time of humanization when mice pups were 1-3 days old, mice were also X-ray irradiated to further prevent immune responses to the transplantation of human CD34$^+$ HSPCs and subsequent blood immune cell reconstitution that would negatively impact the in vivo hematopoiesis assay. Littermates of the same sex were randomly assigned to experimental groups. Mice in the experimental groups were both male and female. Sample sizes are included in Figure 4's legend. No previous procedures were performed on the mice in the experimental groups. Animal research described in the study was approved by the University of Alabama at Birmingham (UAB)'s Chancellor's Animal Research Committee (Institutional Animal Care and Use Committee [IACUC]) and was conducted in accordance with guidelines for housing and care of laboratory animals of the National Institutes of Health and the Association for the Assessment and Accreditation of Laboratory Animal Care International.

Cell lines

The only cell lines cultured in this manuscript are the CD34$^+$ HSPCs isolated from donors' UCB samples for the colony-forming unit (CFU) in vitro hematopoiesis assay. For the assay, isolated CD34$^+$ HSPCs were cultured in methylcellulose media (H4434, StemCell Technologies, Canada) at 37°C, 5% CO$_2$, <90% humidity. The sex of the cells is unavailable because all UCB samples are deidentified. The CD34$^+$ HSPCs are authenticated by the level of CD34 surface expression.

METHOD DETAILS

Isolation of MNCs and CD34$^+$ cell fraction

UCB was collected to a sterile cord blood collection unit (MSC127D, MacoPharma, GA), stored at 4°C until processed, and processed within 24 h of storage. The volume of prepacked citrate phosphate dextrose (35 mL) was subtracted before determining the UCB volume. The MNC fraction was isolated by Ficoll-Paque density gradient centrifugation as reported elsewhere.[70] The numbers of MNC were determined by a TC-10 digital cell counter following mixing 1:40 MNCs:Pharm Lyse (BD Biosciences) and a subsequent 1:2 dilution into 0.4% trypan blue. CD34$^+$ cells in the MNC fraction were positively isolated using CD34 beads (130-046-703, Miltenyi Biotec, Germany) via autoMACS ProCell Separator (Miltenyi Biotec) according to the manufacturer's protocol. Obtained CD34$^+$ cells were counted on TC10 automated cell counter and directly used for downstream applications including flow cytometry and Annexin-V staining with no additional processing. Any leftover CD34$^+$ cells were cryopreserved in liquid nitrogen for other assays.

Flow cytometry

Flow cytometry was performed on a BD FACSymphony (BD medical device, NJ) using a gating strategy shown in Figures S2, S4, S5, and S8 and analyzed using FlowJo 10 (FlowJo, LLC, OR). 100 μL whole UCB was stained with antibodies against human CD3, CD4, CD8, CD14, CD19, CD56, and CD66b and fixed

in RBC Fix & Lysis (422,401, BioLegend, CA), making the total volume 990 μL (total nucleated cell (TNC) fraction). Prior to performing flow cytometry, 10 μL of Precision Count beads (BioLegend) was added for absolute number counting (total volume is 1000 μL) and analyzed using the gating strategy shown in Figure S2. Forty μL of pre- (i.e., MNCs) and post-CD34$^+$ cell isolation fractions were stained with antibodies against human CD34 and analyzed using the gating strategy shown in Figure S4. To determine levels of human lymphocyte reconstitution in humanized mice, 100 μL of peripheral blood was collected via retro-orbital vein at 10 weeks of age and analyzed using the gating strategy shown in Figure S8. Each gate for all flow analysis was determined based on fluorescence-minus one controls (data not shown).

All antibodies were obtained from BioLegend: APC anti-human CD66b (396906, clone QA17A51), PE/Cyanine7 anti-human CD3 (344816, clone SK7), Brilliant Violet (BV) 421 anti-human CD56 (362552, clone 5.1H11), BV510 anti-human CD4 (357420, clone A161A1), BV605 anti-human CD8 (344742, clone SK1), BV711 anti-human CD19 (302246, clone HIB19), BV785 anti-human CD14 (301840, clone M5E2), FITC anti-human CD45 (982316, clone HI30), PE anti-human CD34 (343506, clone 581), APC/Fire750 anti-mouse CD45 (147714, clone I3/2.3). Annexin-V positive apoptotic cells were detected by staining with PE-Annexin-V followed by 7-AAD according to the manufacturer's instructions (Biolegend, 640934) using the gating strategy shown in Figure S5. Due to a requirement of a minimum 0.25 x 10^6 cells for this assay per manufacturer's protocol, we served CD34$^+$ cell samples >0.5 × 10^6 cells obtained following AutoMACS purification in the assay.

Detection of SARS-CoV-2 spike proteins

SARS-CoV-2 spike proteins (S) in UCB plasma samples were not detected by western blotting and immunoprecipitation. For western blotting, plasma samples corresponding to 10 μL of original plasma volume were analyzed on Precast Gel 4–12% (Nacalai USA, CA). S protein was detected with polyclonal Anti-SARS-Related Coronavirus 2 Spike Glycoprotein NR-52947 (BEI resources, VA) at 1/2000 in PBS with 0.02% Tween 20 (PBS-T) and 1% polyvinylpyrrolidone (Millipore Sigma, MA). HRP-conjugated anti-rabbit IgG antibody (R&D, MN) was used at 1/10,000 as a secondary antibody. Pierce ECL Plus Western Blotting Substrate (ThermoFisher Scientific, MA) was used for development, and signals were detected with a Typhoon Trio + Variable Mode Imager (GE Healthcare, GA) and analyzed via ImageJ.

For immunoprecipitation, 3 mL of original UCB plasma was incubated with 100 μL of 10% Protein A/G Magnetic Beads (MedChemExpress, NJ) slurry in the presence of 0.2% CHAPS (Millipore Sigma). As a positive control, one plasma sample negative for anti-SARS-CoV-2 S and N antibodies (N-/S-) and one plasma sample positive for anti-SARS-CoV-2 S antibody (N-/S+) were spiked with 125 ng of recombinant stabilized SARS-CoV-2 S protein (BEI resources) prior to addition of the protein A/G bead slurry. Beads were collected with a magnetic rack (Invitrogen, MA) after 24 h incubation and analyzed via anti-S protein western blotting as above.

Cytokine ELISAs

The concentrations of inflammatory cytokines in the UCB plasma samples were measured by ELISA as described previously, according to the manufacturer's protocols.[71,72] All kits were purchased from ThermoFischer Scientific: IL-6 Human ELISA KIT, High Sensitivity (BMS213HS), IL-8 Human ELISA Kit, Ultra-sensitive (KHC0084), TNF-α Human ELISA Kit, High Sensitivity (BMS223HS), and IFN-γ Human Uncoated ELISA kit (88-7316-88). TNF-α and IFN-γ were less than the detectable/sensitivity level (data not shown).

Detection of SARS-CoV2 S and N antibodies

Anti-SARS-CoV2 N protein antibody was measured by LEGEND MAX SARS-CoV-2 Nucleocapsid Human IgG ELISA Kit (Biolegend). Anti-SARS-CoV2 S protein antibody was detected by using an FDA approved kit for SARS-CoV-2 IgG/IgM rapid antibody tests (AssureTech, MD)

In vitro and *in vivo* hematopoiesis assays

The *in vitro* hematopoiesis assay was performed using methylcellulose media (H4434, StemCell Technologies, Canada) using 1 × 10^3 CD34$^+$ cells as previously described.[48] Three experimental and biological replicates were prepared per donor (n = 7 donors from each group). Each well was bright field imaged with the EVOS M7000 imaging system (ThermoFisher Scientific, MA) at 4× magnification after 14 days and evaluated, according to the methylcellulose manufacturer's protocol. The *in vivo* hematopoiesis assay was

performed by humanization of two immunodeficient mouse strains: NOD.Cg-$Prkdc^{scid}$ $Il2rg^{tm1Wjl}$/SzJ (NSG) and NOD.Cg-$Prkdc^{scid}$ $Il2rg^{tm1Wjl}$ Tg (CMV-IL3, CSF2, KITLG)1Eav/MloySzJ (NSG-SGM3). The transplantation of CD34$^+$ cells into the mice was performed as previously described.[73] Briefly, CD34$^+$ cells (0.1 × 10^6 cells/mouse) from the N-/S- group (4 donors, 10 NSG and 3 NSG-SGM3 mice) and N-/S+ non-vaccinated group (4 donors, 11 NSG and 6 NSG-SGM3 mice) were used for the assay.

Transcriptome analysis

Total RNA was extracted from freshly isolated 1 × 10^6 CD34$^+$ cells using Quick-RNA kits (Zymo Research, CA). High-throughput transcriptome profiles were generated by deep sequencing using Illumina NextSeq 500 (Illumina, CA). The sequence reads that passed quality filters were analyzed by STAR (version 2.7.7a) to align the raw RNA-Seq fastq reads to the human reference genome (GRCh38 p13, Release 36) from Gencode.[74] Following alignment, HTSeq-count (version 0.13.5) was used to count the number of reads mapping to each gene.[75] Normalization and differential gene expression analysis was performed using DE-Seq2[75] with batch correction. Gene ontology (GO) analysis of top differentially expressed genes ($p \leq 0.05$) was performed by using DAVID Bioinformatics Resources.[76] RNA sequencing data are available at GEO: GSE196802.

QUANTIFICATION AND STATISTICAL ANALYSIS

Results are expressed as mean ± standard deviations (SDs). Error bars depict SD. Outliers were removed prior to statistical comparisons via the ROUT method (Q = 5%). Comparisons between multiple groups were performed using an ordinary one-way ANOVA. Comparisons between two groups were performed using an unpaired two-tailed t-test with Welch's correction. All statistical analyses/outlier exclusion were performed using GraphPad Prism 9. n values as well as the statistical analyses and results can be found in the figures/figure legends. A p value less than 0.05 was considered statistically significant. Symbols used in figures as follows: Not significant: ns ($p > 0.05$), * ($p < 0.05$), ** ($p < 0.005$), *** ($p < 0.0005$), and **** ($p < 0.0001$). All enrolled donors with medical records indicating previous or active SARS-CoV-2 infection as determined by COVID-19 PCR assays or SARS-CoV-2 nucleocapsid (N) and/or Spike (S) antigens/proteins in the UCB and validated by the CareStart Rapid COVID-19 antigen test (Intrivo, CA) were excluded from the study.